Z. Kristallogr. Suppl. **26** (2007) 483-488

Diffraction analysis of the lithium battery cathode material $Li_{1.2}Mn_{0.4}Ni_{0.3}Co_{0.1}O_2$

P.S. Whitfield[1,*], I.J. Davidson[1], P.W. Stephens[2], L.M.D. Cranswick[3], I.P. Swainson[3]

[1]Institute for Chemical Process and Environmental Technology, National Research Council, 1200 Montreal Road, Ottawa, Ontario, K1A 0R6, Canada
[2]Department of Physics and Astronomy, SUNY, Stoney Brook, New York, 11794-3800, USA
[3]Canadian Neutron Beam Centre, Chalk River Laboratories, Chalk River, Ontario, K0J 1J0, Canada

[*] Contact author; e-mail: pamela.whitfield@nrc.gc.ca

Keywords: powder diffraction, neutron diffraction, resonant diffraction, constraints

Abstract. In common with many functional materials, the composition of lithium battery cathode materials has become increasingly complex. $Li_{1.2}Mn_{0.4}Ni_{0.3}Co_{0.1}O_2$ is a highly promising cathode material, that can have up to four cations sharing a single site. Determining the occupancies of each individual element requires more information than even a joint X-ray/neutron refinement can provide. For this material additional datasets were taken to exploit changes in elemental contrast that can be induced using resonant diffraction. Together with the actual ratios of Mn:Ni:Co determined using wavelength dispersive XRF, constraints were constructed to allow the transition metals to 'float' across the different cation sites whilst the lithium content could be freely refined. The added complications of a C2/m monoclinic structure and anisotropic broadening made for a very complex refinement. The least squares matrices were examined in order to maintain reasonable ESDs for the variables of interest.

Introduction

Lithium-rich lithium battery cathode materials have been of recent interest due to their promising electrochemical and thermal properties. These materials are effectively a solid solution of Li_2MnO_3 and $LiMO_2$, where M may be one or more metals. Although Li_2MnO_3 is nominally electrochemically inactive, such materials do possess higher capacities than expected when charged to voltages over 4.4V. In addition, Mn^{4+} tends to lend greater thermal stability, and hence the safety characteristics of these materials are potentially better than the industry standard, $LiCoO_2$. The compound described in this paper is effectively a 1:1 solid solution of Li_2MnO_3 and $LiNi_{0.75}Co_{0.25}O_2$, with manganese in the +4 oxidation state and the cobalt and nickel in low-spin +3 states [1].

Lithium battery research has been a fertile area for simultaneous neutron/X-ray structure refinements because of the presence of large amounts of lithium. This has been a powerful approach to localise the elements on particular sites within the structure, due to the differing contrasts between element scattering of X-rays and neutrons. However, in a system with four cations this is insufficient. In common with simultaneous equations, the greater number of cations requires a greater amount of information to solve the puzzle. Two methods for changing the relative scattering powers of the elements are neutron diffraction of isotopically substituted samples and resonant diffraction. The former can be far superior, although the cost involved is often prohibitive.

Resonant diffraction [2, 3] is usually carried out at a synchrotron. It involves tuning the wavelength close to the absorption edge of one of the elements of interest (usually the K edge for transition metals). At this point, that particular element begins to fluoresce, scattering a portion of the incoming radiation inelastically. As the rest of the elements in the sample continue to scatter elastically, the scattering power of that particular element falls with respect to the other elements, as shown in figure 1. The relative change in scattering power depends on how close to the absorption edge the chosen wavelength is located.

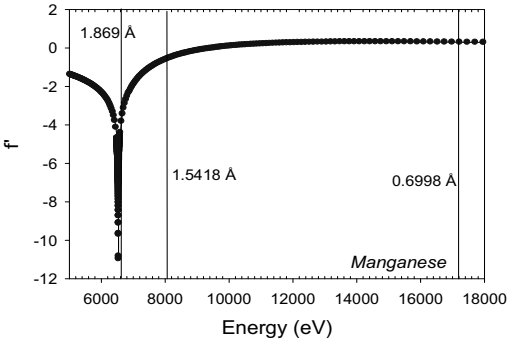

Figure 1. Reduction in scattering power of manganese with changing incident beam energy. Indicated on the graph are the energies for ~MoKα, CuKα and the Mn-edge wavelength used in this paper.

Experimental

The $Li_{1.2}Mn_{0.4}Ni_{0.3}Co_{0.1}O_2$ material was synthesised using a sucrose-based Pechini-like process that has been described previously [1]. Metal nitrates were used as precursors in a sucrose solution with a 4:1 cation:sucrose ratio. The solution was acidified to pH1 using nitric acid. After evaporation of the water, the viscous mixture was carbonised and combusted on the hotplate. The resultant ash was than calcined at 800ºC in air for 6 hours. The transition metal ratios of the prepared material was determined using wavelength-dispersive X-ray fluorescence of a fused borate bead in a Bruker S4 Pioneer spectrometer. A fully calibrated quantitative method was developed due to the severe line overlap and interference.

Neutron diffraction data for structural analysis were collected at room temperature on the NRC DUALSPEC C2 high-resolution neutron powder diffractometer located at the Chalk River Laboratories, Ontario, Canada. The sample was held in a sealed vanadium can and data collected at 1.33Å. The vanadium reflections were included in the neutron refinement as a second phase rather than excluding them. One known instrumental artefact from the detector banks was also excluded. The synchrotron X-ray diffraction data were collected on the X3B1 beamline at the National Synchrotron Light Source at Brookhaven National Laboratory. Data were collected in reflection mode on a quartz zero background at 0.65Å, 1.8932Å and 1.6049Å. The synchrotron datasets correspond to approximately MoKα (off-edge), the MnKα absorption edge and the CoKα absorption edge respectively. Laboratory CuKα is quite close to the CoKα absorption edge, so its inclusion would have been superfluous in this case. The data were analysed using a beta version of Topas 4 (25/4/2006) [4]. Overall thermal parameters were refined for the metal and oxygen sites. Surface roughness was corrected using the algorithm described by Pitschke [5] which allowed reasonable overall thermal parameters to be obtained for the lithium sites.

As the counts obtained for the different datasets were different, weighting was used to balance the contributions of the different datasets to the refinement. The different X-ray datasets were all weighted to give an equal weighting to each. The element contrast for the neutron dataset is much larger than for the resonant scattering datasets, so the neutron dataset a weighting equal to the cumulative counts of all the X-ray datasets.

The constraints for the as-prepared material were constructed such that the overall transition metal ratios remained constant, whilst allowing them to migrate to the lithium sites taking account of different site multiplicities. The concept paralleled that used in GSAS by Joubert *et al* [3], where the transition metals on one particular site are split into portions linked with one of the other cation sites. Given that the starting ratios of the transition ratios are as determined by XRF, the ratios will remain constant despite the presence of a scaling parameter to account for variable lithium content, and the different site multiplicities in the structure. In this manner the occupancies of all the metals were refined simultaneously with the proviso that each site had a total occupancy of 1.0.

Full-pattern anisotropic broadening was fitted using a spherical harmonics convolution of a Lorentzian function. The more severe broadening from $\sqrt{3}a \times \sqrt{3}a$ short range ordering was fitted arbitrarily by application of another Lorentzian profile to specific *hkl* reflections. Although no physical information can be inferred from the profile fitting, it does allow the intensities of the reflections to be modelled more accurately and used within the structural refinement. The A-matrix and correlation matrices were output into the Topas 'out' files to be read into *SVDdiagnostic* [6]. Both the unprocessed and preconditioned matrices were analysed and the generated text file examined for both the condition number and problematic variables.

Results and discussion

The as-prepared material was found by XRF to contain the transition metals in the ratios 48.1% Mn, 38.7% Ni, and 13.1% Co. This is compared to the nominal values of 50% Mn, 37.5% Ni and 12.5% Co.

The structure refinement progressed to a satisfactory fit after fitting the anisotropic broadening. The fits to the 0.65Å data without and with the broadening corrections are shown in

figure 2a and 2b respectively. Although the corrections did not significantly affect the overall lithium to transition metal ratio, it did alter the distribution of transition metals across the cation sites.

The final refined structure for the $Li_{1.2}Mn_{0.4}Ni_{0.3}Co_{0.1}O_2$ with the satisfactory condition numbers is shown in table 1. Some standard uncertainties (SUs) are quite high, but not catastrophic as is the case with quasi singularity. The overall effect of the procedure applied to improve the conditioning was then to reduce large parameter correlations, thereby allowing structural variables to be extracted reliably.

An interesting feature of the structure is that the transition metal occupancies on the *4g* and *2b* sites is far from the random distribution assumed by the average R-3m structure. The lithium-containing *2b* site is nickel-rich whilst the smaller *4g* site is nickel-poor compared to that expected for a random transition metal distribution. This might be expected where nickel is in the +2 oxidation state as the radii of Li^+ and Ni^{2+} are quite close. In this material however, nickel is formally in the low spin +3 oxidation state, and the expected bond length is closer to Mn^{4+} (1.906Å) and low-spin Co^{3+}. Table 2 compares the refined bond lengths with those expected from bond valence considerations. As all published bond valence parameters are for high-spin states, so values for low-spin Co^{3+} and Ni^{3+} were derived from ICSD entries for $LiCoO_2$ and $LiNiO_2$. Values for R_0 were 1.664 and 1.710 for Co^{3+}(LS)-O and Ni^{3+}(LS)-O respectively, which together with a B value of 0.37, leads to octahedral bond lengths of 1.9206 and 1.9664Å. The agreement between the refined and theoretical values is very good, showing that the structure is self-consistent from a crystal chemistry standpoint.

The behaviour of the manganese and nickel appear to be reminiscent of that in the cathode materials $LiMn_{1/2}Ni_{1/2}O_2$ and the lithium-rich $Li[Ni_xLi_{1/3-2x/3}Mn_{2/3-x/3}]O_2$, where $0 \le x \le 0.5$ [7]. The differences in this case are that the nickel is in the low-spin +3 oxidation state as opposed to +2, and cobalt is also present. However, these results suggest that nickel behaves in a similar fashion in both oxidation states. As expected given its relative size, the site preference of low-spin Co^{3+} is between that of Mn^{4+} and Ni^{3+}, although it tends to follow the nickel onto the larger *2b* site in the transition metal layer.

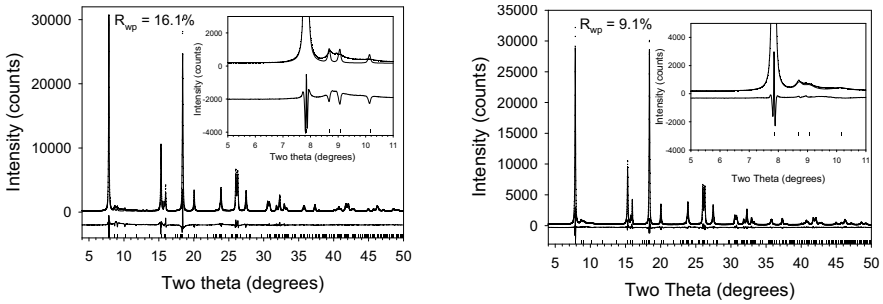

(a) (b)

Figure 2. Fit to the 0.65Å synchrotron data (a) without and (b) with broadening corrections.

Conclusions

The combined neutron and resonant diffraction study has shown that the transition metals in the C2/m Li_2MnO_3-type structure show distinct preference for particular sites. Mn^{4+} preferentially occupies the smaller *4g* site, whilst Ni^{3+} prefers the larger 2b site. Although the bond length of LS-Co^{3+}-O is closer to that of Mn^{4+} than LS-Ni^{3+}, the Co^{3+} shows a preference for the *2b* site. Only nickel has significant occupancy on the lithium sites, despite the fact that it is nominally in the +3 oxidation state in this material. The excess lithium in the transition metal layer, shows a practically 100% selectivity for the *2b* site.

Table 1. Final refined structure of $Li_{1.2}Mn_{0.4}Ni_{0.3}Co_{0.1}O_2$ after a satisfactory condition number had been reached for both the unprocessed and preconditioned matrices. The expected occupancies for a random distribution of transition metal cations are also shown.

SG: C2/m a = 4.98268(23), b = 8.56248(80), c = 5.01340(36) Å, β = 109.2479(95)º
Refined stoichiometry = $Li_{1.165(36)}Mn_{0.402(13)}Ni_{0.323(16)}Co_{0.109(32)}O_2$
Overall residuals: R_{wp} = 9.61%, R_p = 7.0%, Durban-Watson = 1.727

Site	**Atom**	**x**	**y**	**z**	**Occ**	**Occ (random)**	**B_{iso}**
4g M1	Mn	0	0.16597 (14)	0	0.5467(105)	0.4793	0.83(2)
	Ni				0.3345(104)	0.3856	
	Co				0.1152(159)	0.1305	
	Li				0.0036(217)	0.0036	
2b M2	Mn	0	0.5	0	0.1111(93)	0.2152	0.10(6)
	Ni				0.2392(94)	0.1731	
	Co				0.0971(137)	0.0586	
	Li				0.5526(191)	0.5526	
2c Li1	Li	0	0	0.5	0.9966(274)	0.9966	0.96(33)
	Mn				0.0005(133)	0.0016	
	Ni				0.0022(129)	0.0013	
	Co				0.0008(202)	0.0004	
4h Li2	Li	0	0.65505 (384)	0.5	0.9704(139)	0.9704	0.19(17)
	Mn				0.0000(67)	0.0142	
	Ni				0.0296(66)	0.0115	
	Co				0.0000(102)	0.0039	
4i O1	O	0.21918 (57)	0	0.22220 (64)	1	1	0.23(5)
8j O2	O	0.24292 (53)	0.32251 (20)	0.22823 (39)	1	1	1.00(4)

Table 2. Analysis of the refined bond lengths versus the theoretical values based on bond valence parameters.

Bond	Lengths (Å)	Average (Å)	Theoretical bond valence radii (Å)	Difference (Å)
M1 – O1	1.9120(25)	1.9334(45)	1.9287	-0.0047
M1 – O2	1.9127(24), 1.9754(27)			
M2 – O1	2.0503(35)	2.0442(45)	2.0451	+0.0009
M2 – O2	2.0412(21) x2			
Li1 – O1	2.0203(36)	2.1278(45)	2.1284	+0.0006
Li1 – O2	2.1584(19) x2			
Li2 – O1	2.2071(71)	2.1270(99)	2.1242	-0.0028
Li2 – O2	1.9824(64), 2.0952(27)			

References

1. Whitfield, P.S., Niketic, N. & Davidson, I.J., 2005, *J. Power Sources*, **146**, 617.
2. Cox, D.E. & Wilkinson, A.P., 1994, in *Resonant Anomalous X-ray Scattering: Theory and Application*, edited by G. Materlik, C.J. Sparks & K. Fischer (Amsterdam: Elsevier Science).
3. Joubert, J.-M., Cerny, R., Latroche, M., Percheron-Guégan, A. & Yvon, K., 1998, *J. Appl. Cryst.*, **31**, 327
4. Bruker-AXS, *Topas: General Profile and Structure Analysis Software for Powder Diffraction Data*, (Karlsruhe: Bruker-AXS).
5. Pitschke, W., Hermann, H. & Mattern, N., 1993, *Powder Diffraction*, **8**, 74.
6. Mercier, P.H.J, Le Page, Y., Whitfield, P.S. & Mitchell, L.D., 2006, *J. Appl. Cryst.*, **39**, 458.
7. Meng, Y.S., Ceder, G., Grey, C.P., Yoon, W.-S., Jiang, M., Bréger, J. & Shao-Horn, Y., 2005, *Chem. Mater.,***17**, 2386.

Acknowledgements. Work partially funded by the Canadian Department of National Defence and the NRC-AStar Collaborative Research Program.
Research carried out in part at the National Synchrotron Light Source at Brookhaven National Laboratory, which was previously supported by the US Department of Energy, Division of Materials Sciences and Division of Chemical Sciences. The SUNY X3 beamline at NSLS was supported by the Division of Basic Energy Sciences of the US Department of Energy under Grant No. DE-FG02-86ER45231.